



Thermal cracking characteristics of high-temperature granite suffering from different cooling shocks

Yan-jun Shen · Xin Hou · Jiang-qiang Yuan · Shao-fei Wang · Chun-hu Zhao

Received: 24 September 2019 / Accepted: 14 July 2020 / Published online: 7 August 2020
© Springer Nature B.V. 2020

Abstract Cooling shock can be considered a potential method of causing the high-temperature rocks to crack and achieve the most efficient exploitation and utilization of geo-thermal energy in the future. However, it is important to accurately recognize the thermal cracking effect and the corresponding typical characteristics of cooling shock. Therefore, in this study, we conducted a systematic experiment on the effects of cooling shocks with different temperature gradients on the cracking of high-temperature granite. The granite samples were heated to 150, 350, 550, and 750 °C, and then injected with three kinds of refrigerants of 20, 0 and –20 °C into the granite boreholes. Furthermore, the cracking characteristics of granite were compared by means of optical microscope. According to the experimental analysis, several conclusions could be obtained: (1) Compared with natural cooling conditions, cooling shocks of 20, 0, and –20 °C resulted in no evident open cracks on the granite at 150 and

350 °C; however, the distribution of the micro-crack networks became denser with a decrease in the refrigerant temperature. (2) For the high-temperature granite samples at 550 and 750 °C, the effect of the cooling shock was significant, and localized open cracks could be observed; however, several differences were evident in the effect of granite cracking under different combinations of cooling shocks and high temperatures. For granite with the same temperature gradient, with the decrease in the refrigerant temperature, the number of inter-granular and trans-granular cracks increased, and the cooling shock enhanced the cracking effect. (3) The main factor of granite cracking was the anisotropy of the mineral particles affected by the temperature difference, in which a large amount of quartz was contained in the granite, and the effect of repeated phase transformation near 573 °C was remarkable. Moreover, with the temperature difference between the refrigerant and the heated samples increasing, the generated tensile forces in the outer edge of samples would increase rapidly, causing amounts of trans-granular cracks and leading to the denser micro-crack networks. This work can provide an experimental reference for understanding the effect of cooling shock on mechanical properties and cracking of high-temperature rocks.

Y. Shen (✉) · S. Wang
Geological Research Institute for Coal Green Mining,
Xi'an University of Science and Technology, Xi'an
710054, China
e-mail: shenyanjun993@126.com

X. Hou · J. Yuan
School of Architecture and Civil Engineering, Xi'an
University of Science and Technology, Xi'an 710054,
China
e-mail: 17204209083@stu.xust.edu.cn

C. Zhao
Xi'an Research Institute Co. Ltd., China Coal Technology and
Engineering Group Corp., Xi'an 710077, China

Keywords High-temperature granite · Cooling shock · Temperature gradient · Cracking · Mineral particles

1 Introduction

Cooling shock is a common phenomenon in rock engineering under high temperature. In the exploitation of geothermal energy reservoirs, as well as the modes of utilizing geothermal energy, a common method of cooling water injection and hot water extraction is used to gain the geo-thermal resource. During the heat exchange period, cooling shock would occur and cause numerous openings in the high-temperature surrounding rock of the reservoir due to the cooling water injection. These newly produced fractures would greatly affect the extraction process of resources (Dipippo 2016; Kamali and Ghassemi 2018; Kumari et al. 2018a, b; Wang et al. 2019b), and reduce the mechanical properties of bedrock. It is a significant challenge for the further development and utilization of geothermal engineering (Guo et al. 2018; O'Sullivan et al. 2001; Rong et al. 2018). Meanwhile, cooling shock can enhance the cracking rate and increase the heat-exchange speed, which can be regarded as a potential approach to improve the extraction efficiency for the exploitation of geothermal energy reservoirs. Furthermore, some related engineering fields, such as water-spray firefighting in long tunnels and deep-mine cooling by ice-blocks would also be susceptible to similar cooling shocks (Botte and Caspeepe 2017; Belayachi et al. 2019). Therefore, it is necessary to explore the effects of cooling shock on the high-temperature rock and the corresponding thermal cracking characteristics.

It is necessary to understand the mechanical properties of high temperature rock before the depth cognition of the rock thermal cracking phenomenon. As a matter of fact, in recent years, various scholars have carried out a substantial number of laboratory tests on the physical properties of rocks under the high temperature condition. Ersoy et al. (2017) studied the effect of thermal damage on the strength of volcanic rocks, indicating that the strength gradually decreased with an increasing temperature, and a predictive model was used as a function for determining the thermal damage intensity of the rock. Wang et al. (2013) studied the effect of thermal damage on the physical properties of granite. It was found that the permeability of heat-treated samples was four to five orders of magnitude larger than that of intact samples. Zhao (2015) analyzed the problem of thermal-induced micro-cracks reducing the mechanical strength of granite from a microscopic perspective. Studies of high-temperature rock demonstrated that thermal dam-

age gradually accumulated inside the rock owing to high temperatures, eventually leading to a reduction in or even failure of the physical and mechanical properties of the rock (Arafiyo et al. 1997; Freire-Lista et al. 2016; Jin et al. 2019; Peng et al. 2018). Meanwhile, the issue that thermal fracturing of high temperature rock caused by cooling shock has gradually attracted the attention of some relevant scholars. For instance, Isaka et al. (2018) investigated the rapid cooling treatment of granite in water at different temperatures, and they demonstrated that the thermal degradation under rapid cooling was substantially higher than that under slow cooling. Zhang et al. (2018a) analyzed the changes in the physical parameters of granite following heating and rapid cooling. Wu et al. (2019a) has studied the tensile mechanical properties of granite after heating and rapid cooling. It was found that the P-wave velocity of the cooling sample decreased the most, while the tensile strength was the lowest. Based on a study of cooling by means of water, it was found that the cooling method aggravated the weakening of the physical and mechanical properties of high-temperature rock (Han et al. 2019; Hosseini 2017). Furthermore, several scholars have adopted liquid nitrogen to exert a severe cooling method on rocks directly, which also indicated that the physical and mechanical properties of rocks were significantly reduced after cooling shock (Cai et al. 2014, 2015; Gao et al. 2018; Wu et al. 2019b; Wu 2018; Zhang et al. 2018b).

However, the present concerns of these above-mentioned studies mainly focused on the effects on the mechanical properties of high-temperature rocks by different refrigerants. Few investigations have been conducted on the effect of the same refrigerant on the cooling shock cracking considering different temperature gradients. Therefore, in this study, the different cooling shock effects on granite with different temperatures were investigated to demonstrate the differences in the cracking caused by different cooling shocks, and the granite damage under temperature shock was analyzed from a microscope perspective. This study will provide a basic experimental reference for understanding the effect of cooling shock on mechanical properties and cracking of high-temperature rocks.

Table 1 Mineral composition and related parameters of granite

Material	Proportion (%)	Thermal conductivity (W (m K) ⁻¹)	Coefficient of linear expansion (10 ⁻⁶ °C ⁻¹)
Quartz	39.4	7.65	11
Feldspar	53.8	2.33	6
Mica	6.8	1.89	3

2 Experimental preparation and procedure

2.1 Experimental preparation

The samples used in this experiment were granite with uniform granularity, which were obtained from the same rock stratum in Ganzi, Sichuan Province. In the Triassic, Jurassic, Cretaceous and Cenozoic, the magma in Ganzi Prefecture was active, forming a series of intrusive magmatic rock bodies, mostly granite. 85% of the geothermal spots are basically distributed along the periphery of the magmatic rock body or exposed inside, the thermal storage temperature exceeds 200° (267 m), the measured steam temperature of the hot pit reaches 150°. The geothermal resources in Ganzi are characterized by abundant reserves, many beneficial elements, high temperature, shallow burial, etc. However, the dense and complex rock formations have brought challenges to the exploitation of geothermal resources. According to X-ray diffraction analysis, the main mineral components were quartz, feldspar, and mica.

The detailed parameters are displayed in Table 1. The granite was processed into a smooth cube with a side length of 100 mm and drilled in the center of the cube with a rock drilling sampler. The drilling depth was 80 mm and the diameter were 30 mm (The standard for Test and Evaluation of Concrete Compression Strength GB50107–2010. National Standard of P.R.C). The refrigerant used an easily accessible calcium chloride solution (with stable physical properties and low freezing points up to –55 °C), and used the DW-40 type low temperature test box produced by Xinxing Test Instrument Company to reduce the solution to 20 °C, 0 °C, –20 °C, respectively. The adjustable test temperature range was ±40 °C, with an accuracy of ±2%. The instrument for heating the granite was the BLMT-1200 °C high-temperature energy-saving box

furnace, produced by the BLMT Company. The maximum temperature of this muffle furnace can reach 1200 °C, while the error precision is within 2 °C. Moreover, a heating time and constant temperature can be set. To avoid an excessive temperature error in actual operation and understand the temperature state of granite, the AS900B non-contact infrared thermometer produced by the Xima Instrument Company was used for auxiliary verification. Its measuring temperature ranges from –50 °C to 900 °C, with an accuracy of ±2%. The Super-eyes B011 portable electron microscope produced by the Super-eye Technology Company was used to observe the changes in the granite cracks during the later stage. The maximum multiple of the Super-eyes B011 portable electron microscope can identify objects of 14 microns. In addition, Particles Cracks Analysis System (PCAS) fracture analysis software (Liu et al. 2013) is used. Users can automatically segment fracture image after simple operation, complete fracture network recognition and binary parameters of output image, and realize accurate quantitative analysis of fractures.

2.2 Experimental procedure

This experiment focused on the cracking effects of refrigerants on granite with different temperature gradients. The experimental process is illustrated in Fig. 1. Firstly, for the treatment of granite samples, the granite was heated from room temperature (20 °C) to four target temperature by the BLMT-1200 °C high-temperature muffle furnace, namely 150 °C, 350, 550, and 750 °C. Because the heating rate was excessive, cracks in the rock interior would occur to varying degrees. Therefore, the heating rate of the muffle furnace was controlled at 5 °C/min to reach the target temperature (Mallet et al. 2013; OugierSimonin et al. 2011; Zuo et al. 2007). For the treatment of the refrigerant solution, calcium chloride solution exhibits effective fluidity at –20 °C and does not condensate. Therefore, the calcium chloride solution was cooled to three target temperature using the DW-40 cryogenic test chamber, namely 20 °C, 0 °C, and –20 °C. After reaching the target temperature, the entire solution could reach the target temperature for 8 h. Then, the heated granite sample was quickly and carefully removed with tongs and injected into the central drill hole with the prepared calcium chloride solution to fill the drill hole.

The granite samples, with the same temperature gradient, were subjected to three cooling shock tests each time. Moreover, a group of heated granite was subjected to natural cooling (“natural cooling” means the cooling of high-temperature rocks in a muffle furnace that is disconnected from the power supply) as a control group. Without rapid cooling shock treatment, four repeated cooling shock tests of the granite with different temperature were carried out, and a group of naturally cooled granite was used as a control group each time. Test sample numbers are shown in Table 2. Finally, when the granite was cooled to the indoor temperature, the cracks on the outer surface of each group of granite were observed by connecting the Super-eyes B011 electron microscope to a computer.

3 Experimental results and analysis

3.1 Apparent cracking of granite

Following the cooling shock, the surface of each group of high-temperature granite cracked to varying degrees. Although the cracking degree of the natural cooling group as a control group increased with the increase in the granite temperature, compared to the cracking degree of the granite cooling shock groups with the same temperature gradient, the rapid cooling shock enhanced the thermal damage cracking effect, which is consistent with the experimental results of Yang et al. (2017) and Shao et al. (2014). However, the differences in the cooling shocks on the granite cracking were not evident between the 150 °C and 350 °C groups. With the increase in the granite temperature, the differences between the 550 °C and 750 °C groups increased significantly, and the phenomena of powder debris and particle spalling appeared on the sample surfaces. To demonstrate the effect of the cooling shock on the granite cracking, we used particle and crack image recognition and analysis system to process crack images, the main function of the software is to automatically identify particles, pores and fracture images, geometric quantification and statistical analysis (Liu et al. 2011). In addition, to eliminate the influence of the color of the granite minerals on the image recognition, we uniformly sprayed a thin layer of whitewash paint onto the granite surface, to demonstrate the fracturing effects better. The fracturing of granite at different temperatures is displayed in Table 3.

In Table 3, the black surface of the granite represents the cracks and voids. From the comparison of the surface cracking effects in Table 3, it can be observed that the cooling shock had a very poor cracking effect on the 150 °C group, so there was no significant difference among the groups. With the increase in the rock temperature, the differentiation of the cooling shock exhibited evident differences, particularly in the 550 and 750 °C groups. The cracking effect of the cooling shock in the –20 °C group was superior to that in the 0 °C group. The cracking effect of the cooling shock in the 0 °C group was superior to that in the 20 °C group, which was mainly manifested in the cracking area, morphology, and exfoliation of the mineral particles. The data in Fig. 2 indicate the area ratio of the cracks and voids to the total surface, as identified by the software (the area value of the central hole was deducted). Therefore, the effect of the cooling shock cracking can be observed more intuitively from Fig. 2. With the increase in the granite temperature, the differences in the effects of the cooling shock cracking caused by different temperature gradients was more significant, and the cracking effect was also significantly improved owing to the decrease in the cooling shock temperature. Moreover, with the increase in the cooling shock strength, long cracks appeared on the edge of the hole in addition to the cracks on the surrounding boundary. This indicates that the increased cooling shock resulted in a penetrating crack connecting the outer edge of the granite surface to the hole.


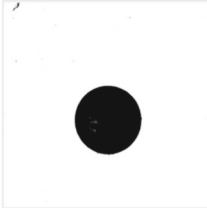
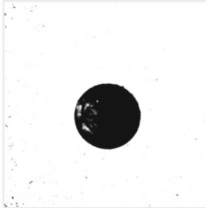
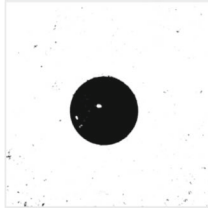
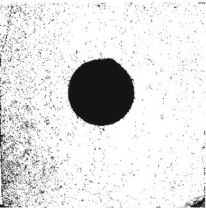
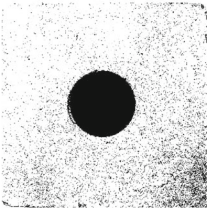
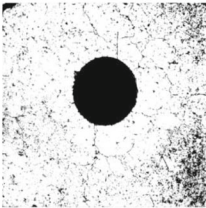
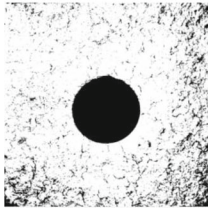
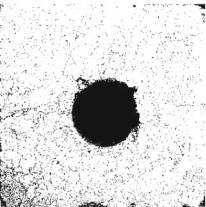
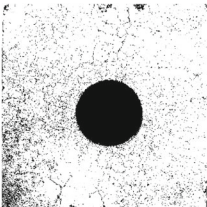
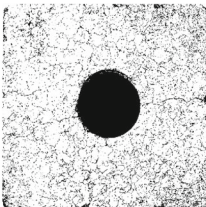
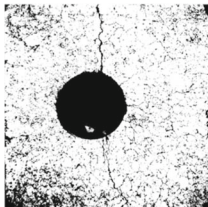
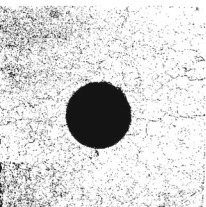
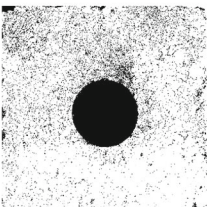
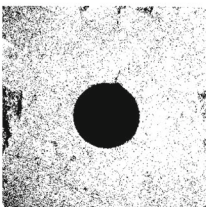
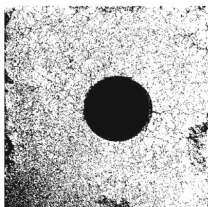
3.2 Microscopic analysis of crack propagation in granite

Following the high temperature and cooling shock treatment, the granite was cooled to room temperature, and the Super-eyes electron microscopy was used to observe the surface cracking of the rock sample. In this study, the crack growth characteristics around and at the boundary of the hole were observed, the crack direction was tracked and spliced, and the general law of the cooling shock cracking was analyzed. No evident cracks were observed on the surfaces of the rock samples at approximately 150 to 350 °C after quenching with refrigerants at the three temperatures, while the mineral particles at 150 °C remained essentially unchanged following the Super-eyes observation, and micro-cracks appeared between certain mineral parti-

Table 2 The test number of granite sample

Granite				
Refrigerant	150 °C	350 °C	550 °C	750 °C
Natural cooling	H150N	H350N	H550N	H750N
20 °C	H150C20	H350C20	H550C20	H750C20
0 °C	H150C0	H350C0	H550C0	H750C0
- 20 °C	H150C-20	H350C-20	H550C-20	H750C-20

Table 3 Comparison of samples surface cracking effects under different cooling shocks

Temperat ure	Natural cooling	Cooling shock 20 °C	Cooling shock 0 °C	Cooling shock -20 °C
150 °C				
350 °C				
550 °C				
750 °C				

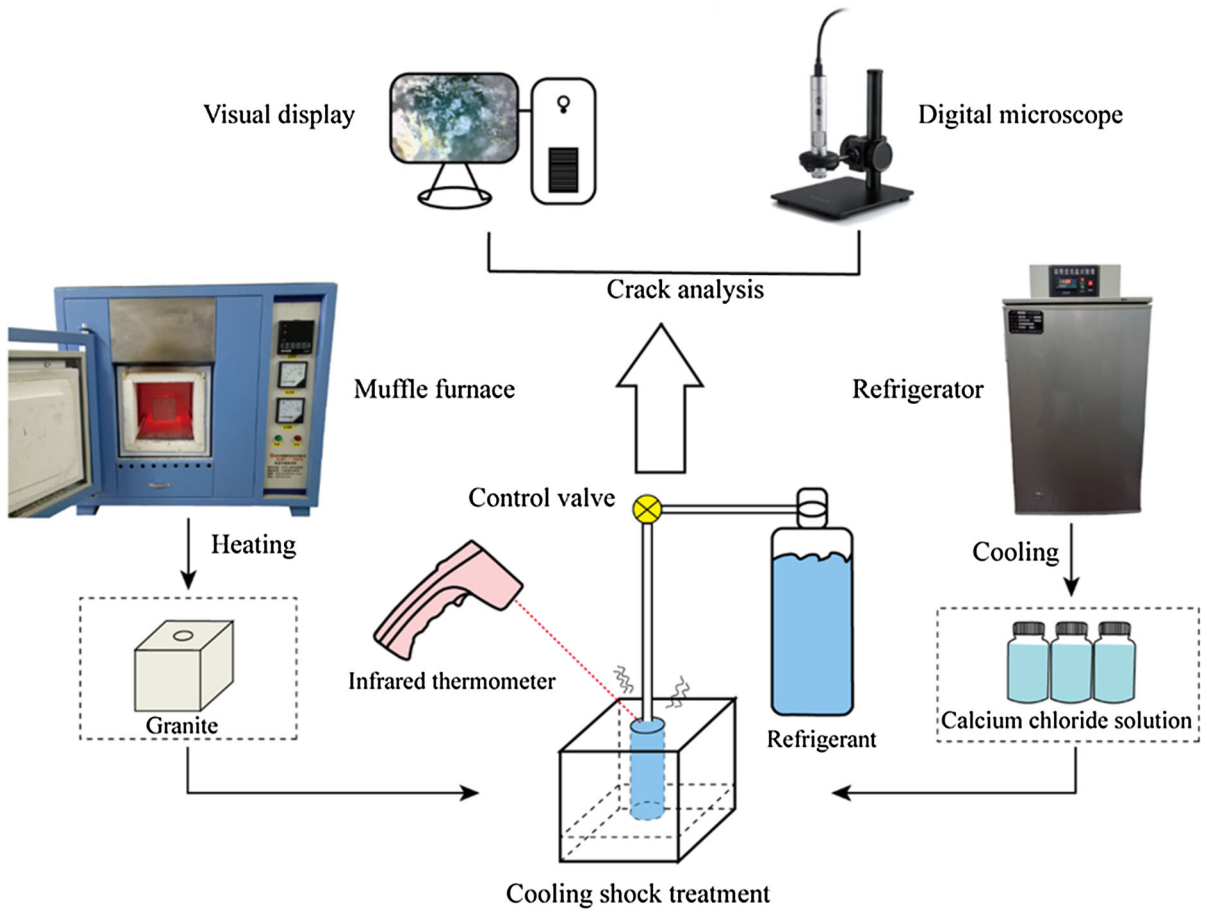
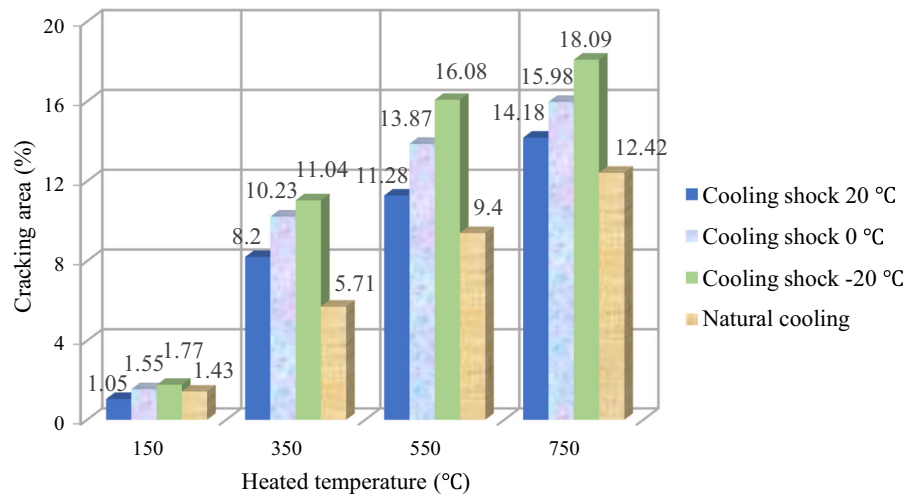


Fig. 1 Diagram of experimental process

Fig. 2 Surface fracturing area ratios of different granite cooling shocks



cles at 350 °C. With an increase in the temperature to 550 and 750 °C, the cold quenching cracking effect of the three temperatures was remarkable. According to the test results, the cooling shock cracking effect of the rock formation at 150 and 350 °C was evidently inferior to that of the rock formation at 550 and 750 °C. In this study, 150 and 350 °C were classified as the low fracture group, while 550 and 750 °C were classified as the high fracture group.

Because the heating temperature of the granite in the 150 °C and 350 °C groups was not very high, following the cooling shock of the three temperature gradients, the cracking conditions of the appearance surfaces could not be observed with the naked eye, so the granite surface condition was observed by the Super-eyes electron microscope. It can be observed from Fig. 3 that, compared to the natural cooling group, the different cooling shocks did not cause cracking of the granite in the 150 °C group. The difference caused by the cooling shock was not exhibited in the granite of the 150 °C group. Up to the temperature threshold of granite cracking, the thermal shock generated was not sufficient to cause the granite to crack. When the temperature increased to 350 °C, followed by a cooling shock, compared to the natural cooling group, it can be observed from the partial enlargement that, after the different cooling shocks, different degrees of fine cracks appeared on the granite surface, and mineral powder appeared in the cooling shock – 20 °C group. One reason that these micro-cracks were produced is because the interior of the rock sample contained initial micropores and original micro-cracks. Moreover, following the high temperature and cooling shock, the mineral particles were deformed. Owing to the inconsistency of the thermal conductivity and linear expansion coefficient of the mineral particles (see Table 1 for the thermal parameters of the mineral components), the particles would exhibit differences after being heated and cooled (Chen et al. 2018; Shen et al. 2018b; Thirumalai and Demou 1974). During the quenching process, with the sudden injection of the refrigerant, the rock instantaneously underwent extremely high temperature changes, and the generated thermal stress destroyed the weakest matrix portion between the connected mineral particles, thereby causing cracks and partial particle peeling between the mineral particles. Under the action of these two aspects, cracks appeared on the granite surface. Furthermore, as a result of the increased temperature difference, the variation caused

by the cooling shock began to become more prominent. As the temperature continued to increase, when the granite was heated to 550 and 750 °C, different types of water inside the rock gradually vaporized and escaped, the mineral composition underwent a phase change and melting reaction, cracks occurred inside, and the surface debris was separated. The cooling shock effect intensified the thermal cracking, and the effects of the different cooling shock cracking were also evident. Cracking of the granite surface could be observed with the naked eye. The photographs of the granite cracking exhibit substandard results, owing to poor light, pixels, and partial small cracks. The surface crack pattern was traced by an electron microscope, and the sketch was used for the reduction. The granite crack appearance is presented in Table 4.

From the crack diagram in Table 4, for the granite with the same temperature gradient, with the decrease in the refrigerant temperature, the cracking effect on the granite was enhanced. Moreover, the crack propagation was extended, additional cracks appeared, and cracking was exhibited along the granite axis. According to the theoretical analysis of the shortest distance of the plastic zone of the composite crack fracture, this energy consumption was the lowest. Moreover, cracks in the cooling shock group appeared from the holes compared to the natural cooling group, and the crack shape became complicated. This indicates that the thermal stress generated by the cooling shock caused more serious damage to the granite, and the varying crack shapes also demonstrated the difference in the cracking effects of the different cooling shocks. The crack morphology was observed by electron microscopy, and the crack propagation is presented in Fig. 4a–d. The mechanism of the rock rupture process can be divided into three successive stages: the ultra-microscopic stage, in which the generation of germination cracks occurs in the entire sample body and the distances between atoms are equivalent; the micro stage, where the crack is equivalent to the structural unit and the defects are formed in the same manner; and the macroscopic stage, in which the crack exceeds an order of magnitude of the structural unit and the micro-cracks merge and develop into a main crack. Fig. 4a–d illustrate the macroscopic stage of the granite fracture, with cracking between the mineral particles. It can be observed from the figure that the crack near the outer boundary was wider, and gradually narrowed in the hole direction. Moreover, the fractures of the 550 °C granite group generally extended

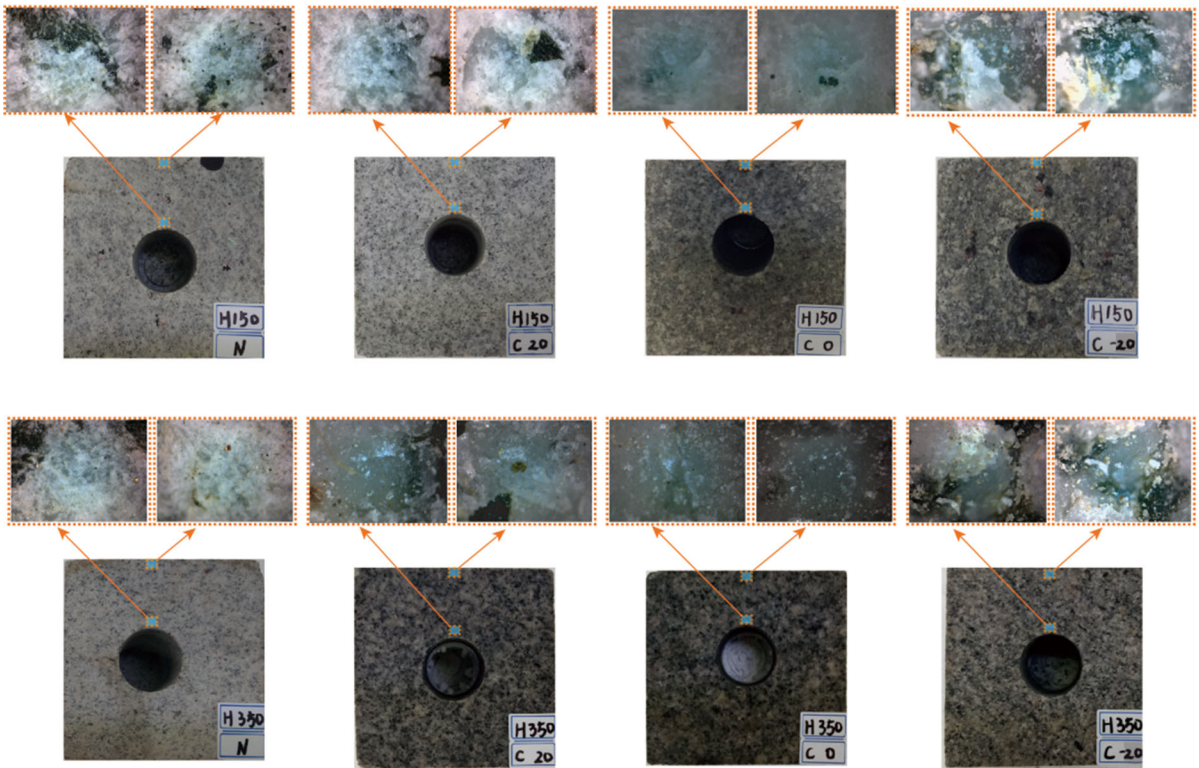


Fig. 3 Comparison of cooling shock effects of granite at 150 and 350 °C

Table 4 Crack characteristics on high-temperature granite surface at 550° and 750° after different cooling shocks

Temperature	Natural cooling	Cooling shock 20 °C	Cooling shock 0 °C	Cooling shock -20 °C
550 °C				
750 °C				

around the mineral particles, resulting in more circumferential cracks. Owing to the huge thermal shock at the surface of the granite group at 750 °C, the circumferential cracks further expanded and penetrated along the grain boundary, eventually forming radial cracks. Furthermore, in the process of the main crack propagation, additional microcrack branches appeared with discrete random distributions, which is associated with the non-uniform microstructures of rocks (Shen et al. 18a; Zhang et al. 2019). Certain mineral particles have higher strength, such as biotite, while some have lower strength, such as quartz. Therefore, under the action of thermal stress, the quartz with a low strength first broke and formed a trans-granular crack. Under the significant thermal shock, some of the black mica also demonstrated the occurrence of trans-granular cracks, and as the cooling shock temperature decreased, the thermal stress increased, and the number of trans-granular cracks also increased, resulting in the rock matrix damage being more serious and being destroyed along the ring direction of the particles. When the thermal expansion coefficient of the matrix is smaller than that of the embedded particles, the matrix and particles are in a stretched state and compressed state, respectively, and the matrix is finally destroyed in the form of radial cracks. When the thermal expansion coefficient of the matrix is larger than that of the embedded particles, the matrix and particles are in the compressive and tensile stress states, respectively, and the matrix is eventually destroyed in the mode of circumferential cracks (Tang et al. 2016).

4 Discussion

The ultimate macroscopic damage of the rock is closely related to its internal microstructure and external load. It undergoes a series of evolution processes, such as microcrack initiation, development, and nucleation. In this experiment, the granite experienced two stages of heat and cold. During this process, the granite minerals changed and the development of cracks appeared macroscopically owing to changes in the internal structure. The analysis of the specific mechanism of the granite crack development can be carried out in terms of the following two aspects.

4.1 Difference analysis of test results

There are some differences between the experimental results of this paper and those of relevant scholars. For example, no cracks are found on the surface of granite at 150 °C, which is consistent with the experimental results of Chen et al. (2017). The microscopic images of granite after different heat treatments are obtained by SEM, and it is found that almost no thermally induced cracks are observed in the samples below 300 °C. However, some scholars have found that cracks will occur in granite below 150 °C, even when heated to 70 °C (Richter and Simmons 1974; Lin 2002). Because of the mineral complexity of granite, the temperature threshold of granite cracking is random and only of statistical significance. In addition, during the natural cooling of granite at 750 °C, there are more micro-crack branches on the surface, showing a discrete random distribution, and a surface cracking area ratio of 15.08%. However, in the study of 700 °C granite natural cooling by Wang Wang et al. 2013, the porosity of the hot cracking specimen is about 3%, but there is no large-scale crack penetration. Compared with the results of this paper, the degree of crack development is smaller, the rock failure degree is lower, and there are no annular cracks in our test. This is due to the fact that the content of quartz with lower strength in granite is 37.9%, which is much higher than 25.8% of Westerly granite, while the content of mica with higher mineral particle strength is only 6.3% lower than 13% of Westerly granite, which results in different cracking differences. Granite is a crystalline rock composed of quartz, feldspar, mica and other minerals. The difference of thermal expansion of each component leads to thermal fracture, and its composition, particle size and cementation degree lead to complex changes in physical properties. When the temperature increases and the local thermal stress is sufficient to meet the necessary conditions for crack formation, thermal fracture occurs. Therefore, for heterogeneous rocks, thermal fracture is random, and the critical temperature of thermal fracture should also be a range. Even the same kind of rock will have thermal fractures in different situations due to the inconsistency of thermal expansion between its cementation conditions, between different particles, between the same particles, between particles and cements, between cements. These thermal cracks may also occur at the beginning of heating, but the quantity and energy are small.

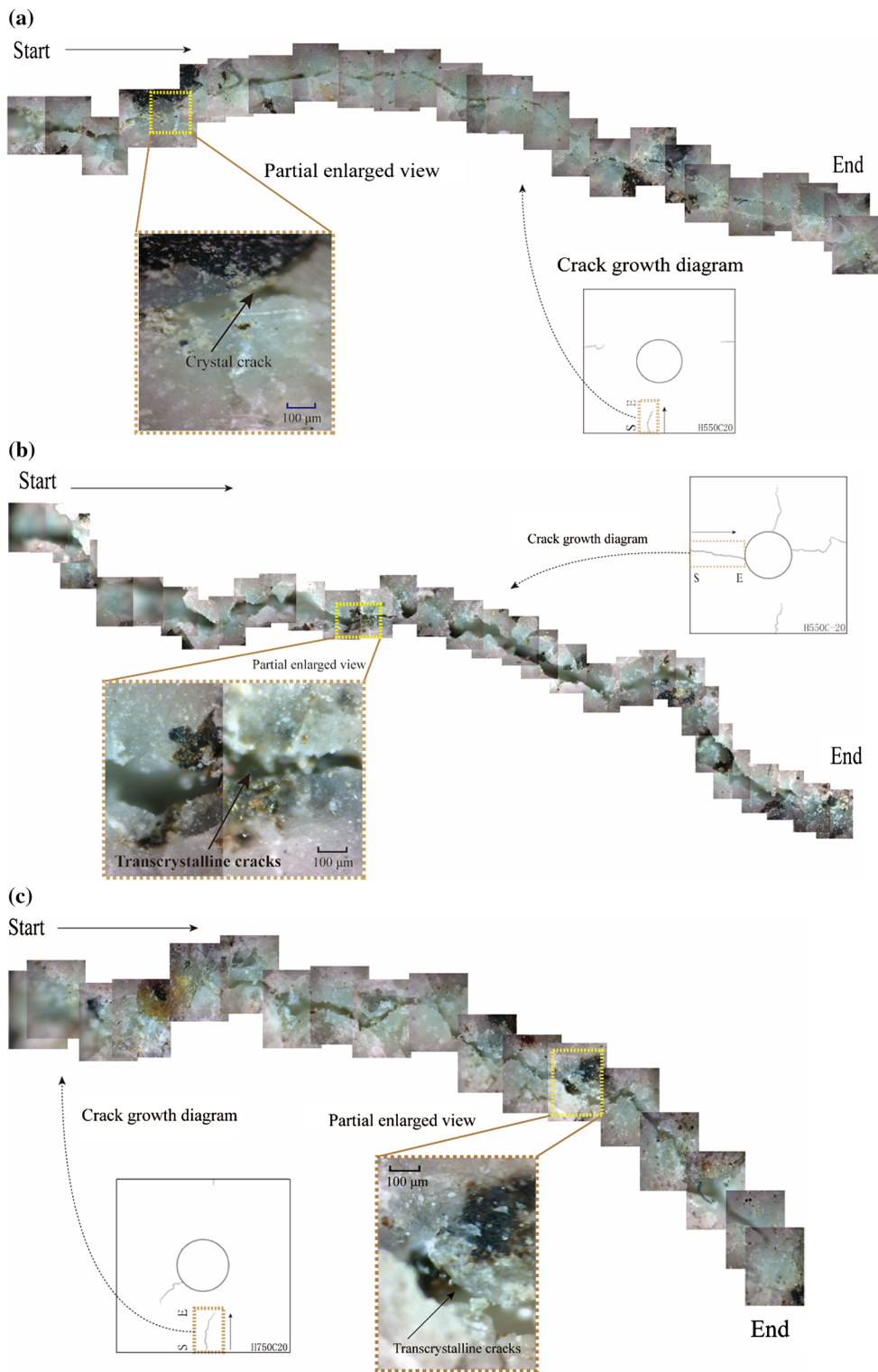


Fig. 4 Cracking extension features of granite samples under different cooling shocks

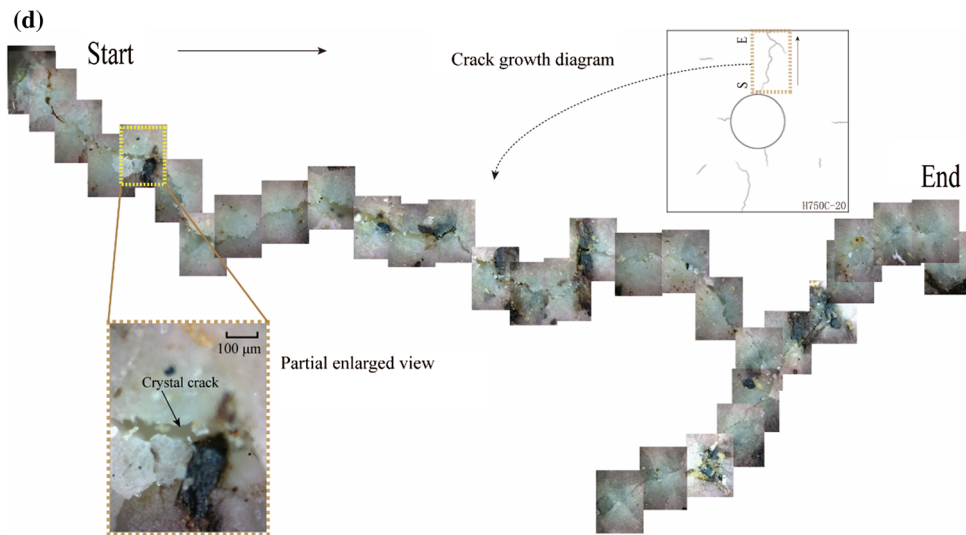


Fig. 4 continued

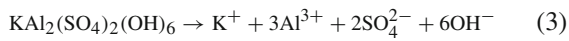
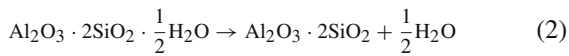
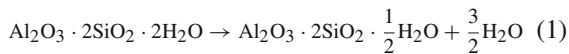
4.2 Analysis of cracking mechanism of cooling shock granite

As the natural granite itself exhibited original defects in the internal structure, when the granite experienced high temperatures, the original micro-cracks developed further and the defects were accelerated to generate thermal cracks, resulting in an irreversible microstructure. The cooling shock also exacerbated this thermal damage. Moreover, the cooling shock effect caused the temperature of the granite outer surface to decrease sharply and the mineral particles to shrink drastically. Although the granite as a whole tended to be in a state of thermal equilibrium owing to heat conduction, the internal temperature of the granite remained high. The thermal stress generated by the temperature difference caused tensile stress on the outer surface of the granite and compressive stress inside (OugierSimonin et al. 2011). When these two stresses exceeded the thermal stress limit of the granite internal structure, new micro-cracks were generated in the sample, and as the refrigerant temperature decreased, the temperature stress generated increased, causing the width and density of the cracks in the granite to increase. Moreover, the development of micro-cracks caused the refrigerant to penetrate further, and the cooling shock again expanded the cracking degree, causing additional thermal cracking.

When high-temperature granite is cooled, the mineral particles shrink sharply, and tensile tangential

stress is formed on the rock surface. When the thermal stress exceeds the thermal stress limit of the structure itself, new micro-cracks are generated in the sample. Because of the different crystalline structure of each mineral component, the thermal stress limit threshold is also different; therefore, the cracking morphology is also different. After the granite is subjected to different cooling shocks, the thermal stress is different, which has become one of the main factors for the difference in rock cracking (Kumari et al. 2018a, b). However, because the thermal stress caused by the temperature difference between the granite and cooling shock was small, the difference in the cooling shock effect between the 150 °C and 350 °C groups was not evident. Moreover, with the increase in the granite temperature, along with the attached water of the internal structure of the granite, the combined water and crystal water decomposed, vaporized, and escaped, and a portion of the mineral physical and chemical reaction occurred (Sun et al. 2016); for example ankerite, pyrite, and kaolinite, among others (as shown by Eqs. 1–4), causing changes in the internal structure of the rock (Just and Kontny 2011). Following the cooling shock, the mineral recrystallized, causing the micropores in the rock to increase further. As the granite temperature and the cooling shock increased, defects gradually accumulated on the surface and interior of the rock sample. The micropores in the rock gradually extended, gathered, and formed connections. Furthermore, although

there were no visible cracks on the surface, the internal structure of the granite changed.



According to the analysis of the granite mineral particles, owing to the anisotropy of the mineral particles themselves, the thermal expansion coefficients of the crystals differed. After the granite experienced high temperatures, the mineral particles were deformed to varying degrees (Mahabadi et al. 2014; Peng et al. 2017), and after suffering from a strong cooling shock effect, the granite mineral particles once again deformed with inconsistency, thereby increasing the rock cracking degree and resulting in the formation of new fissures and further development of the original fissures. In addition to these factors, an uneven thermal expansion coefficient and thermal gradient of the minerals, as well as a non-uniform increase over each mineral component threshold temperature and thermal damage, could also occur (Wang et al. 1989). However, the anisotropic thermal expansion of different minerals has been identified as a main mechanism of thermal cracking (Fredrich and Wong 1986). Moreover, in the stage of approximately 550 to 750 °C, the phase transition of quartz occurred, which is also an important factor causing thermal cracking. Therefore, the performance of the cracking with different cooling shocks in the 550 and 750 °C groups exhibited significant differences. As granite contains more quartz, the quartz will change from the α phase to β phase when heated at 573 °C (Glover 1995). The transformation process of the quartz crystal structure is illustrated in Fig. 5. This transformation process increases the quartz volume. At approximately 8% (Smalley and Marković 2019; Sun et al. 2013), the generation of microfractures and the expansion of aggregation lead to a further increase in the internal defects of granite, and gaps and connections gradually develop. When subjected to cooling shock, as a result of the cooling effect, quartz will change from the β phase to α phase. However, in the actual transformation process, owing to the internal blocking force generated when the lattice structure is deformed, part of the structural deformation is retained when changing back to the original α phase state (Sun et al. 2005; Zhao

et al. 2006). Moreover, the surface energy of quartz becomes very low at the time of two-phase transitions, and cracks are easily generated. Therefore, as the cooling shock temperature was decreased, greater thermal stress was generated and the more severe damage was caused to the mineral particles such as quartz, thereby further increasing the micro-cracks.

4.3 Analysis of cooling shock effect of morphological differences characterizing granite crack mechanisms

After experiencing the initiation, development, extension, and through-connection of micro-cracks, a macroscopic crack is finally formed (Collin and Rowcliffe 2002; Peng et al. 2019). Nasserri used optical methods to show, in detail, the changes of grain boundary and grain boundary crack density with temperature in granite (Nasserri et al. 2009), which provided a basis for the formation and development of internal cracks in granite. From the perspective of mineral energy, this paper analyzes when the high-temperature granite encountered a sudden cooling shock, the thermal stress generated by the significant temperature gradient first tore the weakly connected matrix (rock bridge) between the mineral particles, and progressed along the mineral particles to form inter-granular fracture, as illustrated in Fig. 6a. The formation and decomposition of mineral crystals are related to the lattice energy. The order in which the minerals are crystallized from the dissociation dispersion system should follow the order in which the lattice energy is reduced. The location of microcracks is related to the type of minerals, and microcracks at grain boundaries usually occurring between minerals with lower lattice energy. It can be observed from Table 5 that the feldspar and quartz lattice energy was lower and the black mica lattice energy was higher. When a large temperature difference produces a thermal stress greater than the cementation force between mineral particles, inter-granular cracks are generated, and propagate along weaker grains. With a further reduction in the cooling shock temperature, when the mineral particles could not withstand this thermal stress, the low lattice energy quartz and feldspar particles were first broken, followed by the high lattice energy of the crystal biotite fracturing, and the connections and combinations of the cracks gradually developed into a trans-granular crack,

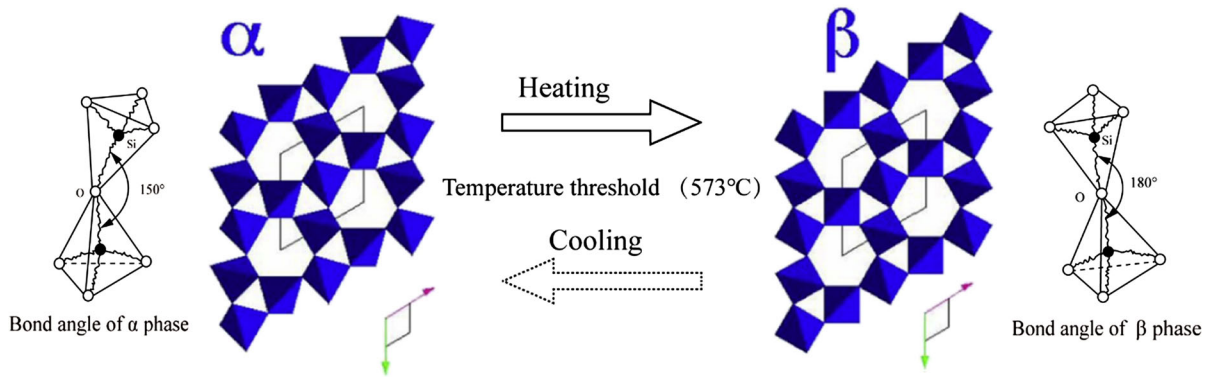


Fig. 5 Transition process of quartz- α to quartz- β (573°)

as indicated in Fig. 6b. Furthermore, cracks developing during the expansion of the local stress concentration phenomenon is very significant. In particular, a stress concentration is formed in the tip region of the crack. During the process of rapid expansion, when the crack encounters the particle interface or mineral particles with higher lattice energy, it will change the advancement direction, and then develop along the longitudinal and lateral directions, changing from one-dimensional line damage to two-dimensional surface damage, thereby forming a large microcrack damage area (Wang et al. 2019a, 2018; Zhao et al. 2019). The original grain, crystal plane, microcrack, joint, and discontinuous and other structures led to an uneven local stress distribution, which increased the speed of the local defect formation, causing the distribution of uneven micro-cracks. Micro-cracks that were diffusely distributed in the damaged area continuously gathered and merged, and finally formed macroscopic cracks.

5 Conclusions

In this experiment, granite samples with different temperatures were subjected to different cooling shock effects, and the cracking effects and crack morphologies were compared from a mesoscopic point of view, which highlighted the differences owing to the varying temperature gradients. Moreover, the cracking mechanism caused by the cooling shock was analyzed. The main conclusions are as follows:

(1) There is no significant difference in the macroscopic cracking effects of granite at 350°C and below with different cooling shocks. With the increase in the

granite temperature, when the temperature is higher than 550°C , the thermal damage of granite increases owing to the anisotropy of the mineral particles and repeated phase transformation of quartz, while the cooling shock effect enhances the cracking. Moreover, the difference in the cracking caused by different temperature gradients gradually becomes evident, and with the decrease in the cooling shock temperature, the granite cracks that appear on the macroscopic scale are more significant.

(2) At a granite temperature of 350°C and below, under different cooling shocks, the matrix (“rock bridge”) between the grains first ruptures. The crack propagates along the grain and the crack development is mainly dominated by inter-granular cracks, accompanied by a uniform distribution of network micro-cracks. At a granite temperature of 550°C and above, under different cooling shocks, as the cooling shock temperature decreases, the resulting tensile force increases, which is sufficient to destroy the lattice energy of the mineral particles, and these sequentially break in the order of lattice strength. The number of trans-granular cracks increases continuously, and the number of network micro-cracks also becomes denser.

(3) The experimental results demonstrate that different cooling methods have a significant influence on rock cracking. A lower refrigerant temperature results in a higher granite temperature, and with a greater temperature difference between the two, additional cracks appear in the granite, and the cracks propagate and extend more fully. Therefore, temperature shock can be used as an effective means of rock breaking, and it can appropriately increase the temperature difference to improve the efficiency of breaking hard rock. It can

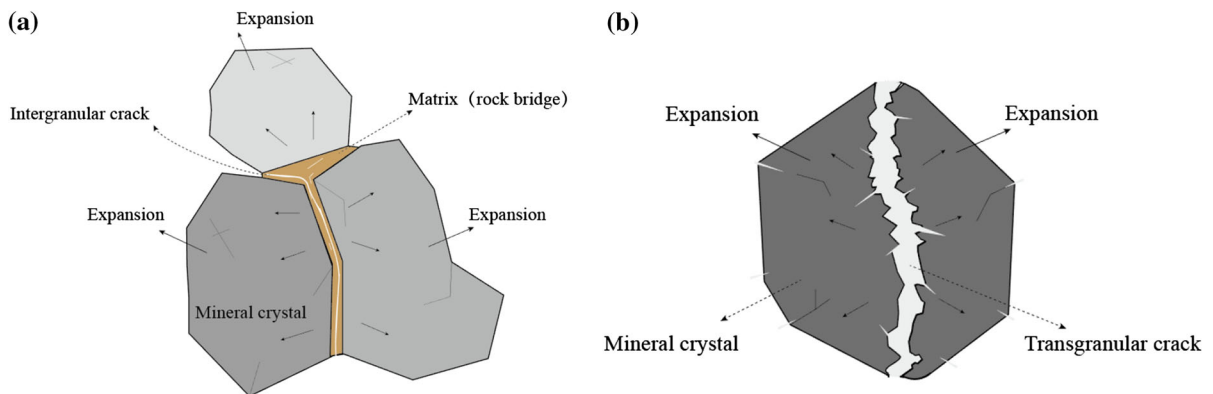


Fig. 6 The generalized model for two cracking characteristics of granite sample. **a** Inter-granular crack. **b** Trans-granular crack

Table 5 Lattice energy of several common minerals

Mineral particles	Peridot	Pyroxene	Amphibole	Black mica	Feldspar	Quartz
Lattice energy (kcal/g)	4.2	4.1	3.8	3.	2.4	2.6

be applied in engineering fields such as the establishment of geothermal reservoirs, oil drilling, and tunnel fire assessment.

Acknowledgements This work was financially supported by the National Natural Science Foundation of China (No. 41772333) and the Open Fund of State Key Laboratory of Frozen Soil Engineering (No. SKLFSE201713).

Compliance with Ethical Standards

Conflict of interest On behalf of all authors, the corresponding author states that there is no conflict of interest.

References

- Arafijo RGS, Sousa JLAO, Bloch M (1997) Experimental investigation on the influence of temperature on the mechanical properties of reservoir rocks. *Int J Rock Mech Min Sci* 34(3–4):298
- Belayachi N, Mallet C, Marzak EI, M. (2019) Thermally-induced cracks and their effects on natural and industrial geomaterials. *J Build Eng* 25:100806. <https://doi.org/10.1016/j.job.2019.100806>
- Botte W, Caspee R (2017) Post-cooling properties of concrete exposed to fire. *Fire Saf J* 92:142–150. <https://doi.org/10.1016/j.firesaf.201706.010>
- Cai C, Li G, Huang Z, Shen Z, Tian S, Wei J (2014) Experimental study of the effect of liquid nitrogen cooling on rock pore structure. *J Nat Gas Sci Eng* 21:507–517. <https://doi.org/10.1016/j.jngse.2014.08.026>
- Cai C, Li G, Huang Z, Tian S, Shen Z, Fu X (2015) Experiment of coal damage due to super-cooling with liquid nitrogen. *J Nat Gas Sci Eng* 22:42–48. <https://doi.org/10.1016/j.jngse.2014.11.016>
- Chen L, Wang A, Suo X, Hu P, Zhang X, Zhang Z (2018) Effect of surface heat transfer coefficient gradient on thermal shock failure of ceramic materials under rapid cooling condition. *Ceram Int* 44:8992–8999. <https://doi.org/10.1016/j.ceramint.2018.02.100>
- Chen SW, Yang CH, Wang GB (2017) Evolution of thermal damage and permeability of Beishan granite. *Appl Therm Eng* 110:1533–1542
- Collin M, Rowcliffe D (2002) The morphology of thermal cracks in brittle materials. *J Eur Ceram Soc* 22:435–445
- Dippio R (2016) *Geothermal power plants principles. Application, case studies and environmental impact*, 3rd edn. Elsevier, Amsterdam
- Ersoy H, Kolayli H, Karahan M, Harputlu Karahan H, Sünnetci MO (2017) Effect of thermal damage on mineralogical and strength properties of basic volcanic rocks exposed to high temperatures. *Bull Eng Geol Environ* 78:1515–1525. <https://doi.org/10.1007/s10064-017-1208-z>
- Fredrich JT, Wong T (1986) Micromechanics of thermally induced cracking in three crustal rocks. *J Geophys Res Solid Earth* 91:12743–12764. <https://doi.org/10.1029/JB091iB12p12743>
- Freire-Lista DM, Fort R, Varas-Muriel MJ (2016) Thermal stress-induced microcracking in building granite. *Eng Geol* 206:83–93. <https://doi.org/10.1016/j.enggeo.2016.03.005>
- Gao F, Cai C, Yang Y (2018) Experimental research on rock fracture failure characteristics under liquid nitrogen cooling conditions. *Results Phys* 9:252–262. <https://doi.org/10.1016/j.rinp.2018.02.061>
- Glover PWJ et al (1995) α/β phase transition in quartz monitored using acoustic emissions. *Geophys J Int* 120:775–782

- Guo L, Zhang Y, Zhang Y, Yu Z, Zhang J (2018) Experimental investigation of granite properties under different temperatures and pressures and numerical analysis of damage effect in enhanced geothermal system. *Renew Energy* 126:107–125. <https://doi.org/10.1016/j.renene.2018.02.117>
- Han G, Jing H, Su H, Liu R, Yin Q, Wu J (2019) Effects of thermal shock due to rapid cooling on the mechanical properties of sandstone. *Environ Earth Sci*. <https://doi.org/10.1007/s12665-019-8151-1>
- Hosseini M (2017) Effect of temperature as well as heating and cooling cycles on rock properties. *J Mining Environ* 8:631–644. <https://doi.org/10.22044/jme.2017.971>
- Isaka B, Gamage R, Rathnaweera T, Perera M, Chandrasekharan D, Kumari W (2018) An influence of thermally-induced micro-cracking under cooling treatments: mechanical characteristics of Australian. *Granite Energies* 11:1338. <https://doi.org/10.3390/en11061338>
- Jin P, Hu Y, Shao J, Zhao G, Zhu X, Li C (2019) Influence of different thermal cycling treatments on the physical, mechanical and transport properties of granite. *Geothermics* 78:118–128. <https://doi.org/10.1016/j.geothermics.2018.12.008>
- Just J, Kontny A (2011) Thermally induced alterations of minerals during measurements of the temperature dependence of magnetic susceptibility: a case study from the hydrothermally altered Soultz-sous-Forêts granite. *France Int J Earth Sci* 101:819–839. <https://doi.org/10.1007/s00531-011-0668-9>
- Kamali A, Ghassemi A (2018) Analysis of injection-induced shear slip and fracture propagation in geothermal reservoir stimulation. *Geothermics* 76:93–105. <https://doi.org/10.1016/j.geothermics.2018.07.002>
- Kumari WGP, Ranjith PG, Perera MSA, Chen BK (2018) Experimental investigation of quenching effect on mechanical, microstructural and flow characteristics of reservoir rocks: thermal stimulation method for geothermal energy extraction. *J Petrol Sci Eng* 162:419–433. <https://doi.org/10.1016/j.petrol.2017.12.033>
- Lin W (2002) Permanent strain of thermal expansion and thermally induced microcracking in Inada granite. *J Geophys Res Solid Earth* 107(B10):ECV3
- Liu C, Shi B, Zhou J, Tang C (2011) Quantification and characterization of microporosity by image processing, geometric measurement and statistical methods: application on SEM images of clay materials. *Appl Clay Sci* 54:97–106. <https://doi.org/10.1016/j.clay.2011.07.022>
- Liu C, Tang CS, Shi B, Suo WB (2013) Automatic quantification of crack patterns by image processing. *Comput Geosci* 57:77–80
- Mahabadi OK, Tatone BSA, Grasselli G (2014) Influence of microscale heterogeneity and microstructure on the tensile behavior of crystalline rocks. *J Geophys Res Solid Earth* 119:5324–5341. <https://doi.org/10.1002/2014jb011064>
- Mallet C, Fortin J, Gueguen Y, Bouyer F (2013) Effective elastic properties of cracked solids: an experimental investigation. *Int J Fract* 18(2):275–282
- Nasseri M, Schubnel A, Benson P, Young R (2009) Common evolution of mechanical and transport properties in thermally cracked westerly granite at elevated hydrostatic pressure. *Rock Phys Nat Hazards* 166(5–7):927–948
- O'Sullivan MJ, Pruess K, Lippmann MJ (2001) State of the art of geothermal reservoir simulation. *Geothermics* 30:395–429
- Ougier-Simonin A, Gueguen Y, Fortin J, Schubnel A, Bouyer F (2011) Permeability and elastic properties of cracked glass under pressure. *J Geophys Res* 116(B07)
- Peng J, Rong G, Tang Z, Sha S (2019) Microscopic characterization of microcrack development in marble after cyclic treatment with high temperature. *Bull Eng Geol Environ*. <https://doi.org/10.1007/s10064-019-01494-2>
- Peng J, Rong G, Yao M, Wong LNY, Tang Z (2018) Acoustic emission characteristics of a fine-grained marble with different thermal damages and specimen sizes. *Bull Eng Geol Environ*. <https://doi.org/10.1007/s10064-018-1375-6>
- Peng J, Wong LNY, Teh CI (2017) Influence of grain size heterogeneity on strength and microcracking behavior of crystalline rocks. *J Geophys Res Solid Earth* 122:1054–1073. <https://doi.org/10.1002/2016jb013469>
- Rong G, Peng J, Cai M, Yao M, Zhou C, Sha S (2018) Experimental investigation of thermal cycling effect on physical and mechanical properties of bedrocks in geothermal fields. *Appl Therm Eng* 141:174–185. <https://doi.org/10.1016/j.applthermaleng.2018.05.126>
- Richter D, Simmons G (1974) Thermal expansion behavior of igneous rocks. *Int J Rock Mech Min Sci Geomech* 11:403–411
- Shao S, Wasantha PLP, Ranjith PG, Chen BK (2014) Effect of cooling rate on the mechanical behavior of heated Strathbogie granite with different grain sizes. *Int J Rock Mech Mining Sci* 70:381–387. <https://doi.org/10.1016/j.ijrmms.2014.04.003>
- Shen Y, Yang Y, Yang G, Hou X, Ye W, You Z, Xi J (2018a) Damage characteristics and thermo-physical properties changes of limestone and sandstone during thermal treatment from –30°C to 1000°C. *Heat Mass Transf* 54:3389–3407. <https://doi.org/10.1007/s00231-018-2376-5>
- Shen Y, Zhang Y, Gao F, Yang G, Lai X (2018b) Influence of Temperature on the Microstructure Deterioration of Sandstone. *Energies* 11:1753. <https://doi.org/10.3390/en11071753>
- Smalley I, Marković SB (2019) Controls on the nature of loess particles and the formation of loess deposits. *Quatern Int* 502:160–164. <https://doi.org/10.1016/j.quaint.2017.08.021>
- Sun Q, Zhang W, Su T, Zhu S (2016) Variation of wave velocity and porosity of sandstone after high temperature. *Heat Acta Geophys* 64:633–648. <https://doi.org/10.1515/acgeo-2016-0021>
- Sun Q, Zhang Z, Xue L, Zhu S (2013) Physico-mechanical properties variation of rock with phase transformation under high temperature. *Chin J Rock Mech Eng* 32:935–942
- Sun Q, Zhao Z, Zhang P, Jing H, Meng C (2005) Modification mechanism of properties of hot-reclaimed quartz sands. *Foundry*:87–88
- Tang SB, Zhang H, Tang CA, Liu HY (2016) Numerical model for the cracking behavior of heterogeneous brittle solids subjected to thermal shock. *Int J Solids Struct* 80:520–531. <https://doi.org/10.1016/j.ijsolstr.2015.10.012>
- Thirumalai K (1974) Thermal expansion behavior of intact and thermally fractured mine rocks. *AIP Conf Proc*. <https://doi.org/10.1063/1.2945937>
- Wang D, Sun L, Wei J (2019a) Microstructure evolution and fracturing mechanism of coal under thermal shock. *Rock Soil Mech* 40529:529–538

- Wang D, Zhang P, Pu H, Wei J, Liu S, Yu C, Sun L (2018) Experimental research on cracking process of coal under temperature variation with industrial micro-CT. *Chin J Rock Mech Eng* 37:2243–2252
- Wang G, Liu G, Zhao Z, Liu Y, Pu H (2019b) A robust numerical method for modeling multiple wells in city-scale geothermal field based on simplified one-dimensional well model. *Renew Energy* 139:873–894. <https://doi.org/10.1016/j.renene.2019.02.131>
- Kumari WGP, Ranjith PG, Perera MSA, Chen BK (2018) Experimental investigation of quenching effect on mechanical, microstructural and flow characteristics of reservoir rocks: thermal stimulation method for geothermal energy extraction. *J Pet Sci Eng* 162:419–433. <https://doi.org/10.1016/j.petrol.2017.12.033>
- Wang HF, Bonner BP, Carlson SR, Kowallis BJ, Heard HC (1989) Thermal stress cracking in granite. *J Geophys Res* 94:1745. <https://doi.org/10.1029/JB094iB02p01745>
- Wang X, Schubnel A, Fortin J, Guéguen Y, Ge H (2013) Physical properties and brittle strength of thermally cracked granite under confinement. *J Geophys Res Solid Earth* 118:6099–6112. <https://doi.org/10.1002/2013jb010340>
- Wu Q, Weng L, Zhao Y, Guo B, Luo T (2019a) On the tensile mechanical characteristics of fine-grained granite after heating/cooling treatments with different cooling rates. *Eng Geol* 253:94–110. <https://doi.org/10.1016/j.enggeo.2019.03.014>
- Wu X, Huang Z, Cheng Z, Zhang S, Song H, Zhao X (2019b) Effects of cyclic heating and LN₂-cooling on the physical and mechanical properties of granite. *Appl Therm Eng* 156:99–110. <https://doi.org/10.1016/j.applthermaleng.2019.04.046>
- Wu X et al (2018) Investigation on the damage of high-temperature shale subjected to liquid nitrogen cooling. *J Nat Gas Sci Eng* 57:284–294. <https://doi.org/10.1016/j.jngse.2018.07.005>
- Yang S, Ranjith PG, Jing H, Tian W, Ju Y (2017) An experimental investigation on thermal damage and failure mechanical behavior of granite after exposure to different high temperature treatments. *Geothermics* 65:180–197. <https://doi.org/10.1016/j.geothermics.2016.09.008>
- Zhang F, Zhao J, Hu D, Skoczylas F, Shao J (2018a) Laboratory investigation on physical and mechanical properties of granite after heating and water-cooling treatment. *Rock Mech Rock Eng* 51:677–694. <https://doi.org/10.1007/s00603-017-1350-8>
- Zhang S, Huang Z, Wang H, Zhang H, Zhang C, Xiong C (2018b) Thermal characteristics analysis with local thermal non-equilibrium model during liquid nitrogen jet fracturing for HDR reservoirs. *Appl Therm Eng* 143:482–492. <https://doi.org/10.1016/j.applthermaleng.2018.07.088>
- Zhang Y, Wong LNY, Chan KK (2019) An extended grain-based model accounting for microstructures in rock deformation. *J Geophys Res Solid Earth* 124:125–148. <https://doi.org/10.1029/2018jb016165>
- Zhao Z (2015) Thermal influence on mechanical properties of granite: a microcracking perspective. *Rock Mech Rock Eng* 49:747–762. <https://doi.org/10.1007/s00603-015-0767-1>
- Zhao Z, Dou Z, Xu H, Liu Z (2019) Shear behavior of Beishan granite fractures after thermal treatment. *Eng Frac Mech* 213:223–240. <https://doi.org/10.1016/j.engfracmech.2019.04.012>
- Zhao Z, Sun Q, Zhang P, Jing H, Sun Y (2006) Effect of calcination on phase transformation and expansibility of quartz sands during heating. *Foundry*:961–964
- Zuo J, Xie H, Zhou H, Peng S (2007) Experimental research on thermal cracking of sandstone under different temperature. *Chin J Geophys* 04:1150–1155

Publisher's Note Springer Nature remains neutral with regard to jurisdictional claims in published maps and institutional affiliations.